Evolution of the Post-Collision-Interaction Profile from the Resonant Auger Shakeup/Shakedown Lines at the Ionization Threshold

H. Aksela, M. Kivilompolo, E. Nõmmiste, and S. Aksela
Department of Physical Sciences, University of Oulu, Linnanmaa, FIN-90570 Oulu, Finland
(Received 5 June 1997)

Xe $4d_{5/2}$ and Kr $3d_{5/2}$ Auger spectra were studied by scanning the photon energy across the corresponding ionization thresholds. Finest details in the development of the post-collision-interaction profile from the shakeup/shakedown lines were observed experimentally for the first time. The utilization of the resonant Auger Raman effect allowed one to resolve, with very high resolution, new intense fine structures besides the conventional $np \rightarrow mp$ shake transitions in the shake features. They were identified to be due to the transitions to the ms and $(m-1)d$ type final states. [S0031-9007(97)04798-4]

PACS numbers: 32.80.Hd, 32.80.Fb

When the photon energy increases approaching the core ionization threshold, the resonant excitations to the Rydberg states and the adjacent decay processes take place most probably via the resonant Auger process. Especially for the excitations to higher Rydberg states very strong shakeup/shakedown structures are found besides the spectator resonant Auger lines (see, e.g., [1–7]). On the other hand, when the photon energy is scanned from the high energy side to the ionization threshold, the well known post-collision-interaction (PCI) effects, shift in the peak position and increasingly asymmetric line shape, are observed in the normal Auger electron lines (see, e.g., [8–11]). A gradual evolution of the PCI profile from the shake structure takes place when the photon energy crosses the threshold. This transition has been of great interest to both the experimentalists (see, e.g., [6,7,11–13]) and the theoreticians [12–14] but the problem has not yet been solved in detail with a satisfactory way. Above the threshold, the potential curve models of PCI lead to surprisingly accurate predictions. The shake calculations, emerging from the quantum-mechanical treatment, work well when crossing the threshold. At higher resonances the shake model predicts prominent oscillations in shake probabilities [4]. No effect of this is seen when detecting the evolution of the PCI profile. Experimental resolution, however, has so far been insufficient to resolve all the finest details in the shake modified Auger line profile around the threshold.

Recent rapid progress in the performance of the synchrotron radiation instrumentation resulting in higher photon fluxes and better energy resolutions of the monochromators and the electron spectrometers provides completely new possibilities to study this transition phenomenon experimentally in much more detail than before. When the photon bandwidth is smaller than the lifetime broadening of the core excited state, one can benefit from the Auger resonant Raman effect [12,15]. Then the observed resonant Auger linewidths are practically determined only by the photon band and the spectrometer broadening in addition to the Doppler broadening. Therefore, the resonant Auger line can be made much narrower than the lifetime width of the core excited states, which sets the lower limit for the widths of the normal Auger electron lines.

In this Letter we shall report new very high resolution results for the Xe $4d$ and Kr $3d$ threshold Auger spectra when the photon energy is scanned from the region of the conventional resonance excitations to the PCI region. The spectra are discussed in the frame of the shake model for the resonant Auger process versus the conventional PCI model for the normal Auger process. New previously undetected structures, which do not obey the monopole transition selection rules, are also observed to accompany the monopole shake transitions. Their existence manifests that not only the sharing of energy but also the exchange of angular momentum takes place between the electrons involved in the process.

The measurements were carried out at the Finnish beam line [16] of MAX-laboratory, in Lund, Sweden. Synchrotron radiation for the beam line at 550 MeV MAX I storage ring is generated by a short period undulator [17], and it is monochromatized by the modified SX-700 plane grating monochromator [18]. The ultimate photon energy resolution is in the order of 6–10 meV (FWHM) for the photon energy range of 65–95 eV used in this study. The applied electron spectrometer system [19] includes the Scienta-200 hemispherical analyzer [20] which can be rotated around the direction of the photon beam. The spectra of this study were recorded, however, with the fixed "magic angle" of 54.7°. The relatively low flux of the second generation MAX I storage ring was partly compensated by the use of the special gas cell and the position sensitive multidetection of the spectrometer. The ultimate resolution of the spectrometer in the electrically noisy synchrotron radiation laboratory environment was about 10 meV. With reasonable intensity the Xe $4d_{5/2}^{-1}np$ and Kr $3d_{5/2}^{-1}np$ resonant Auger spectra showed the total widths of 30–40 meV, which are still 3–4 times smaller than the lifetime widths of the corresponding core exited states. This resolution

 0031-9007/97/79(25)/4970(4)$10.00

enables one to observe completely new fine structures in the spectra.

The electron spectra following the decay of the Xe $4d_{5/2}^{-1}np$, εp, and Kr $3d_{5/2}^{-1}np$, εp threshold excitations are represented in Figs. 1 and 2, respectively. The photon energy was varied in the ranges of 65–68 and 91–95 eV for xenon and krypton, respectively. Note that the Xe $4d_{5/2}^{-1}$ and Kr $3d_{5/2}^{-1}$ ionization limits are at 67.548 and 93.788 eV, respectively [21]. The spectra of the Auger electrons were recorded in the kinetic energy range near the Xe $5p^{-2}(^1S_0)$ and Kr $4p^{-2}(^1S_0)$ singlet parent lines where the structure of the spectra should be the simplest.

The first striking feature in the series of the spectra is that the peak structure is very rich and is getting tighter and tighter when the photon energy is approaching the ionization limit. The manifold of the most intensive lines for each photon energy is done by the spectator resonant Auger lines and their many shakeup and shakedown lines. The transitions, e.g., for Xe are of the type $4d^9np \rightarrow 5p^{-2}(^1S_0)mp$, $m = n, n \pm 1, n \pm 2, \ldots$. The peaks which correspond to the spectator resonant Auger transition without the adjacent shake process are of minor strength in most of the spectra. m values as high as 16 are discernible. Note that in optical data the energy levels $5p^{-2}(^1S_0)mp$, $m = 6$ are the highest ones reported in the literature [22].

A gradual evolution of the manifold peak structure to the broad PCI-type shape takes place when the photon energy crosses the threshold. The formation of the PCI shape is nicely demonstrated already below the threshold by connecting the peak maxima. The overall line shape is fairly well reproduced by the semiclassical or classical PCI models (see, e.g., [23,24]). It was demonstrated previously by Schmidt [9] that, for instance, for Xe at $h\nu = 67.80$ eV the model of Russek and Mehlhorn [23] gives an excellent agreement with experiment. However, even with photon energies greater than the ionization energy, sharp peaks, due to the recapture of the photoelecton, are seen at the lower binding energy side of the PCI profile. The potential curve models of the PCI are not capable of reproducing any sharp peak structure.

For the theoretical description which accounts for the fine structure as well, we refer to the time-independent scattering theory [14,25]. The transition matrix element which describes the photoexcitation and Auger decay as a one-step process is then given by

$$T_{\beta\alpha} = \langle \psi_\beta^- H_{\rm int} \psi_\alpha \rangle + \sum_\tau \int \frac{\langle \psi_\beta^- | H - E | \psi_\tau \rangle \langle \psi_\tau | H_{\rm int} | \psi_\alpha \rangle}{\hbar\omega - \hbar\omega_\tau + i\Gamma_\tau/2} . \quad (1)$$

Here H is the total Hamiltonian operator, E is the total energy, and $H_{\rm int}$ is the operator of the photon-electron interaction. The intermediate-state wave function ψ_τ contains an excited electron in a bound or in a continuum state that is coupled to the ionic state with one core hole. The final-state scattering wave function ψ_β^- includes one electron in the continuum and another electron in either a discrete excited state or in a low-energy continuum state.

Several approximations have been introduced in the literature to overcome the difficulties in numerical computations. These include the factorization of the many-electron interaction amplitude into the overlap element $\langle nlj \,|\, mlj \rangle$ and the Auger decay amplitude. The latter is, furthermore, approximated to remain constant within the resonant Auger/PCI region as the kinetic energy of Auger electrons is changing only slightly.

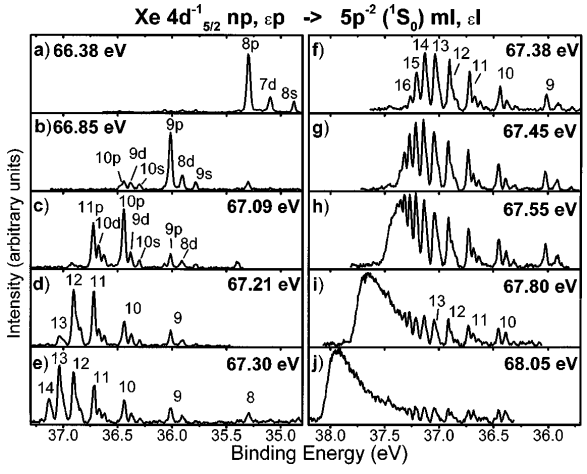

FIG. 1. Kinetic energy region of the $4d_{5/2}^{-1}np \rightarrow 5p^{-2}(^1S_0)ml$ transitions in Xe taken with photon energies corresponding to (a) the $4d_{5/2} \rightarrow 7p$, (b) the $4d_{5/2} \rightarrow 8p$, (c) the $4d_{5/2} \rightarrow 9p$, (d) the $4d_{5/2} \rightarrow 10p$ excitations, and (e)–(g) the higher excitations overlapping with each other. Photon energies above the $4d_{5/2}$ ionization threshold were used when recording the spectra (h)–(j).

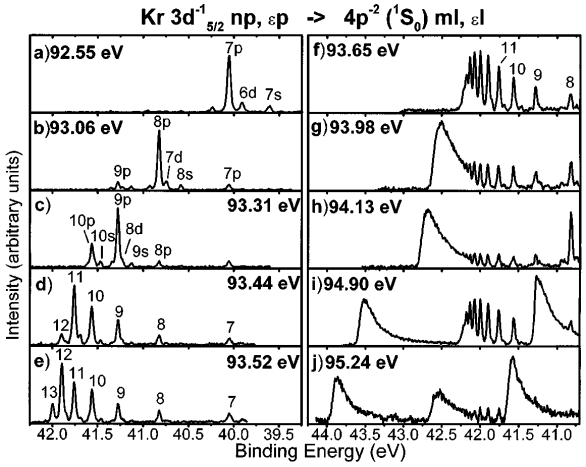

FIG. 2. Kinetic energy region of the $3d_{5/2}^{-1}np \rightarrow 4p^{-2}(^1S_0)ml$ transitions in Kr taken with photon energies corresponding to (a) the $3d_{5/2} \rightarrow 6p$, (b) the $3d_{5/2} \rightarrow 7p$, (c) the $3d_{5/2} \rightarrow 8p$, (d) the $3d_{5/2} \rightarrow 9p$ excitations, (e) and (f) the excitations to higher states overlapping with each other, and (g)–(j) excitations above the $3d_{5/2}$ ionization limit. The structure at around 42 eV in (i) and at around 42.5 eV in (j) is due to the $3d_{3/2}^{-1}np \rightarrow 4p^{-2}(^1S_0)ml$ transitions and the structure on its lower binding energy side is due to the $3d_{5/2}^{-1}np \rightarrow 4p^{-2}(^1D_2)ml$ transitions.

Close to the resonance the second term in (1) dominates. As long as the lifetime width Γ is much less than the spacing of the intermediate states, only one state contributes in the summation. The first five resonances in Kr and Xe serve as good examples here. The ratio of spectator/various shake transitions, predicted by the overlap of the Dirac-Fock (DF) or Hartree-Fock (HF) wave functions, agrees well with the experimental values at the first three resonances. The DF results were reported previously [1,2], and the HF calculations, carried out now using the wave functions generated with the code of Cowan [26], gave very similar results. At the fourth resonance ($np = 8p$ for Kr and $np = 9p$ for Xe), however, the spectator and shakedown contributions are clearly underestimated by the shake theory. The shake predictions do not differ much for Kr and Xe, either. The experiment, however, indicates that the shakeup to the overnext state is clearly lower in case of Kr as compared to Xe. A similar tendency is seen when passing to the next resonance ($np = 9p$ for Kr and $np = 10p$ for Xe). Even though the shake calculations predict a similar behavior, the shakeup to the overnext state has reached a clear maximum in Kr, but in Xe the next and overnext states are almost equally populated. From here on the maximal shakeup turns to favor the spectator and shakedown transitions. In Xe the turning point is reached earlier than in Kr. As the spacing of Rydberg states becomes less than Γ, more and more states are involved, and interference of the channels leading to the same final state takes place. It was demonstrated recently by Armen and co-workers that, in a case similar to this [27], a coherent summation of amplitudes of various paths is needed to correctly reproduce the experiment. Strictly speaking, the language of spectator/shake/recapture lines loses its meaning, and thus should be considered only as a tentative assignment even if used through the work.

Because of a high probability for transitions populating final states with mlj, $m = n - 1, n - 2, \ldots$, at higher resonances, the maximum of the spectral distribution shifts from what is predicted by the spectator model solely. The kinetic energies increase from the nominal resonant/normal Auger energies, in accordance with the PCI model. As the $|nlj\rangle$ is already in the continuum, the $|mlj\rangle$ may still be bound (which was for the first time demonstrated quantum mechanically for Ar by Tulkki *et al.* [25]). A "recapture" of the photoelectron takes place, resulting in peaks which show a Raman narrowing. Since only discrete final states are available instead of a continuous distribution on final state energies, the energy conservation prevents the broadening of the recapture lines. The transitions to final states above the double ionization threshold are characterized by Lorentzian line shapes. For transitions to states at threshold, a cutoff of the Lorentzian distribution should exist. Because of the heavy overlap of the transitions to the states around the threshold the evolution of the individual line shapes is not discernible in the experimental spectra.

The second very interesting feature in the experimental spectra is that each of the spectator/shake peak is composed of several components. This is clearly seen, e.g., for Xe $10p$ and $11p$ lines [see, e.g., Fig. 1(c)] which seem to be formed from three components. For higher m values the splitting is decreasing rapidly and appearing as asymmetric line shapes. Our interpretation for this triplet structure is that besides the $5p^{-2}(^1S_0)mp$ final states also the $5p^{-2}(^1S_0)ms$ and $(m - 1)d$ states are populated in the course of the resonant Auger process. This interpretation is supported by the present multiconfiguration DF (MCDF) calculations, in comparison with earlier results by Hansen and Persson [22], for the final state energies as follows: The MCDF calculations were first carried out for the $5p^{-2}6p$, $5p^{-2}5d$, and $5p^{-2}6s$ configurations of Xe. In a comparison with previous results from the optical measurements [22] the calculations were found to reproduce the order and the splitting of the $5p^{-2}(^1S_0)6p$, $5p^{-2}(^1S_0)5d$, and $5p^{-2}(^1S_0)6s$ levels fairly well. There were lines (65–68, 50–51, and 40 in [28]) in the $4d^{-1}6p$ resonant Auger spectrum for which the energy separation agreed very well. The most intense component in the spectrum with highest binding energy was thus identified to be due to the transitions to the $5p^{-2}(^1S_0)6p$ state, and the less intense components on its low energy side to the $5p^{-2}(^1S_0)5d$ and the $5p^{-2}(^1S_0)6s$ states, respectively. The calculations predict a decrease in the splitting in passing to configurations with spectator electron at higher and higher Rydberg states. This is consistent with the experimental finding. Note that our previous analysis in Ref. [1] was insufficient in assigning the fine structures around the $5p^{-2}(^1S_0)np$, $n = 7$, 8, and 9 states.

None of the final states belonging to $5p^{-2}ms$ and $5p^{-2}(m - 1)d$ configurations are allowed to be populated via conventional shake modified resonant Auger transitions, as the shaking of the electron is allowed by the monopole transition selection rules only. The $5p^{-2}mp$, and the $5p^{-2}(m - 1)d$ and $5p^{-2}ms$ configurations are of different parities which prevents the mixing between them via the final ionic state configuration interaction (FISCI). Therefore, FISCI is ruled out in producing the triplet peak structure. In principle, the $5p^{-2}(m - 1)d$ and $5p^{-2}ms$ type of configurations could be fed via the direct valence photoionization or the participator Auger decay to the $5s^{-1}5p^6(^2S_{1/2})$ state which is further redistributed to the main and satellite lines due to the strong FISCI. However, the total angular momentum values of the observed $5p^{-2}(^1S_0)\,(m - 1)d$ states are $3/2$ and $5/2$. Thus, as the FISCI is limited to those with the same total angular momentum value ($J = 1/2$) only, the $5p^{-2}(^1S_0)\,(m - 1)d, J = 3/2$ and the $5p^{-2}(^1S_0)\,(m - 1)d, J = 5/2$ states are not allowed to mix with the $5s^{-1}5p^6(^2S_{1/2})$ state. Hence, both the direct photoionization and the participator decay cannot explain the finding alone.

In our spectra, the strength of the lines with $5p^{-2}(^1S_0)\,(m - 1)d$ and $5p^{-2}(^1S_0)ms$ character closely follows that of the $5p^{-2}(^1S_0)mp$ states. For instance,

in Fig. 1(a) the $5p^{-2}(^1S_0)8d$ and $5p^{-2}(^1S_0)9s$ states are hardly discernible but the $5p^{-2}(^1S_0)7d$ and $5p^{-2}(^1S_0)8s$ states are strong, whereas it is just opposite in Fig. 1(b). The numerical values of 0.26 and 0.18 and of 0.15 and 0.09 were observed for the intensity ratios $(m-1)d$ to mp and ms to mp in Xe and Kr, respectively. These are the average values; note the large variations in the ratios at different resonances [compare, e.g., Figs. 1(b) and 1(c)].

Our observation indicates that it is not only the resonant Auger decay of the type $4d_{5/2}^{-1}np_{3/2}, J=1 \rightarrow 5p^{-2}(^1S_0)mp_{3/2}\varepsilon d_{5/2}, J=1$ that gives rise to the structures in the spectra, but there are also transitions like $4d_{5/2}^{-1}np_{3/2}, J=1 \rightarrow 5p^{-2}(^1S_0)md_{5/2}\varepsilon p_{3/2}, J=1$, where the exchange of the angular momenta of the excited and ejected electrons has taken place. In all the predictions reported so far in the literature, the channel interaction has been considered as of minor importance and thus omitted. Channel interaction could, however, influence not only the exchange of energy but also the exchange of angular momenta. Here we may consider the following possibility as an example: The participator Auger decay/direct photoionization channel $5s_{1/2}^{-1}\varepsilon p_{3/2}, J=1$ is mixed via final continuum state configuration interaction (FCSCI) with the $5s^25p^{-2}(^1S_0)5d_{5/2}\varepsilon p_{3/2}, J=1$ and the $5s^25p^{-2}(^1S_0)6s_{1/2}\varepsilon p_{3/2}, J=1$ continuum channels. In addition, these channels mix with the $5p^{-2}(^1S_0)6p_{3/2}\varepsilon d_{5/2}, J=1$ channel, populated heavily by the spectator Auger decay of the virtual intermediate $4d_{5/2}^{-1}6p_{3/2}, J=1$ state. Hence, the final ionic state $5s^25p^{-2}(^1S_0)5d_{5/2}$, $J=5/2$ could get fed via such a mixing at resonance photon energies. It is, however, a complicated task to include channel interactions like this in the calculations, especially as there are many more channels to be included.

From the experimental finding here it is clear that shake modified Auger resonant Raman description, even though including the coherence between the paths through all the intermediate states, fails to reproduce the finest details of experiment. Exchange of angular momentum plays a more prominent role than expected before. More theoretical work is needed to arrive at a description that correctly reproduces the finest details in the now observed evolution of the Auger line shape when crossing the threshold.

We are grateful to the members of our group, especially to Dr. O.-P. Sairanen and to Mr. J. Karvonen, for their contribution in the earlier stage of the experimental work. The staff of MAX-laboratory is also acknowledged for assistance during the beam time. This work has been supported financially by the Research Council for Natural Sciences of the Academy of Finland, the Emil Aaltonen Foundation, and Suomen Kultuurirahaston Pohjois-Pohjanmaan Rahasto.

[1] O.-P. Sairanen, H. Aksela, S. Aksela, J. Mursu, A. Kivimäki, A. Naves de Brito, E. Nõmmiste, S. J. Osborne, A. Ausmees, and S. Svensson, J. Phys. B **28**, 4509 (1995).

[2] J. Jauhiainen, H. Aksela, O.-P. Sairanen, E. Nõmmiste, and S. Aksela, J. Phys. B **29**, 3385 (1996).

[3] H. Aksela, S. Aksela, H. Pulkkinen, G. M. Bancroft, and K. H. Tan, Phys. Rev. A **37**, R1798 (1988).

[4] S. B. Whitfield, J. Tulkki, and T. Åberg, Phys. Rev. A **44**, R6983 (1991).

[5] H. Aksela, S. Aksela, A. Mäntykenttä, J. Tulkki, E. Shigemasa, A. Yagishita, and Y. Furusawa, Phys. Scr. **T41**, 113 (1992).

[6] . D. Čubrić, A. A. Wills, J. Comer, and M. A. MacDonald, J. Phys. B **25**, 5069 (1992).

[7] D. Čubrić, A. A. Wills, E. Sokell, J. Comer, and M. A. MacDonald, J. Phys. B **26**, 4425 (1993).

[8] V. Schmidt, N. Sandner, W. Mehlhorn, M. Y. Adam, and F. Wuilleumier, Phys. Rev. Lett. **38**, 63 (1977).

[9] V. Schmidt, Z. Phys. D **2**, 275 (1996).

[10] M. Borst and V. Schmidt, Phys. Rev. A **33**, 4456 (1986).

[11] G. B. Avaldi, R. I. Hall, G. Dawber, P. M. Rutter, and G. C. King, J. Phys. B **24**, 427 (1991).

[12] G. B. Armen, T. Åberg, J. C. Levin, B. Crasemann, M. H. Chen, G. E. Ice, and G. S. Brown, Phys. Rev. Lett. **54**, 1142 (1985).

[13] J. A. de Gouw, J. van Eck, J. van der Weg, and H. G. M. Heideman, J. Phys. B **28**, 1761 (1995).

[14] T. Åberg, Phys. Scr. **T41**, 71 (1992).

[15] A. Kivimäki, A. Naves de Brito, S. Aksela, H. Aksela, O.-P. Sairanen, A. Ausmees, S. J. Osborne, J. B. Dantas, and S. Svensson, Phys. Rev. Lett. **71**, 4307 (1993).

[16] S. Aksela, A. Kivimäki, A. Naves de Brito, O.-P. Sairanen, S. Svensson, and J. Väyrynen, Rev. Sci. Instrum. **65**, 831 (1994); S. Aksela, A. Kivimäki, O.-P. Sairanen, A. Naves de Brito, E. Nõmmiste, and S. Svensson, Rev. Sci. Instrum. **66**, 1621 (1995).

[17] H. Ahola and T. Meinander, Rev. Sci. Instrum. **63**, 372 (1992); Å. Andersson, S. Werin, T. Meinander, A. Naves de Brito, and S. Aksela, Nucl. Instrum. Methods Phys. Res., Sect. A **362**, 586 (1995).

[18] S. Aksela, A. Kivimäki, R. Nyholm, and S. Svensson, Rev. Sci. Instrum. **63**, 1252 (1992).

[19] S. Svensson, J.-O. Forsell, H. Siegbahn, A. Ausmees, G. Bray, S. Södergren, S. Sundin, S. J. Osborne, S. Aksela, E. Nõmmiste, J. Jauhiainen, M. Jurvansuu, J. Karvonen, P. Barta, W. R. Salaneck, A. Evaldson, M. Lögdlund, and A. Fahlman, Rev. Sci. Instrum. **67**, 2149 (1996).

[20] N. Martensson, P. Baltzer, P. A. Brühwiler, J.-E. Forsell, A. Nilsson, A. Stenborg, and B. Wannberg, J. Electron Spectrosc. Relat. Phenom. **70**, 117 (1994).

[21] G. C. King, M. Tronc, F. H. Read, and R. C. Bradford, J. Phys. B **10**, 2479 (1977).

[22] J. E. Hansen and W. Persson, Phys. Scr. **36**, 602 (1987).

[23] A. Russek and W. Mehlhorn, J. Phys. B **19**, 911 (1986).

[24] P. van Straten, R. Morgenstern, and A. Niehaus, Z. Phys. D **8**, 35 (1988).

[25] J. Tulkki, T. Åberg, S. B. Whitfield, and B. Crasemann, Phys. Rev. A **41**, 181 (1990).

[26] R. D. Cowan, *The Theory of Atomic Structure and Spectra* (University of California Press, Berkeley, 1981).

[27] G. B. Armen, J. C. Levin, and I. A. Sellin, Phys. Rev. A **53**, 772 (1996).

[28] H. Aksela, O.-P. Sairanen, S. Aksela, A. Kivimäki, A. Naves de Brito, E. Nõmmiste, J. Tulkki, A. Ausmees, S. J. Osborne, and S. Svensson, Phys. Rev. A **51**, 1291 (1995).